Research Article Vol. 12, No. 4 / 1 Apr 2022 / Optical Materials Express 1417
Optical Materials EXPRESS

Photonic synaptic system for MAC operations by interconnected vertical cavity surface emitting lasers

JOSHUA ROBERTSON, JUAN ARTURO ALANIS, MATĚJ HEJDA, AND ANTONIO HURTADO*

Institute of Photonics, Dept. of Physics, University of Strathclyde, Glasgow, UK
**antonio.hurtado@strath.ac.uk*

Abstract: We report experimentally on high-speed, tuneable photonic synaptic architectures realized with vertical cavity surface emitting lasers (VCSELs) connected in series and in parallel configurations. These are able to perform the controlled weighting of fast (150 ps long) and low energy (μW peak power) optical pulses (or spikes), and permit high-speed (0.5 GHz) dynamic weight tunability, for the implementation of important spike processing functionalities. These include, for the in-series VCSEL synaptic architecture, the performance of accumulative weighting and, due to amplification, the compensation of losses in sequential neural network layers. Additionally, for the in-parallel VCSEL synaptic architecture, we show the system's ability to perform key multiply and accumulate operations using fast, low-power optical spiking signals as inputs. Moreover, this work uses off-the-shelf VCSELs operating at key telecom wavelengths (1300 and 1550 nm) thus making our technique fully compatible with optical telecommunication networks and data centre technologies. These results therefore highlight the suitability of our approach for hardware-friendly, low power, high-speed and fast tuning VCSEL-based photonic synaptic architectures with excellent scalability prospects for use in future neuromorphic photonic computing systems.

1. Introduction

Neuromorphic (brain-like) computing platforms have seen a sharp rise in development over recent years. This follows significant interest in machine learning (ML) and artificial intelligence (AI), fields that have been instrumental in the realization of systems that impact our daily lives, including pattern recognition platforms, computer vision technologies, etc [1]. Neuromorphic computing takes direct inspiration from the way information is processed by the networks of biological neurons in the brain. There are major ongoing efforts in both academic and industrial sectors focused on development of neuromorphic systems in traditional CMOS-based technologies [2–4]. While simultaneously, the push for novel photonic approaches to neuromorphic systems is gaining more interest thanks to their viability for surpassing the limitations of electronic components. Without the requirement for large power-intensive chips and electronic signal routing, photonic platforms may represent a technology which can yield faster operation speeds, with smaller reduced footprint systems and higher bandwidth [5,6]. Hence, in recent years new photonic approaches have emerged for the development of artificial photonic neural networks (PNNs) and the ultrafast emulation of neuron-like behaviour. These have been based on a wide range of photonic systems, such as phase change materials (PCMs) [7], microring weight banks [8], modulators [9] and semiconductor lasers [10–12]. Among the latter approaches, vertical cavity surface emitting lasers (VCSELs) are attracting increasing interest. VCSEL-neurons in particular have demonstrated their ability to reproduce, yet at ultrafast sub-nanosecond rates, the dynamical

#450923 https://doi.org/10.1364/OME.450923
Journal © 2022 Received 10 Dec 2021; revised 4 Feb 2022; accepted 15 Feb 2022; published 10 Mar 2022

Optical Materials EXPRESS

spike firing behaviour of biological neurons, with the ability to operate as integrate-and-fire neuronal models [13,14] and communicate using spiking responses [15–17]. These breakthroughs were subsequently utilized to demonstrate the ability of VCSEL-based spiking neurons to perform complex processing tasks, such as optical convolution [18] and pattern recognition [13] for the spike-based processing of images and binary patterns at ultrafast rates. Photonic reservoir computers based upon VCSELs, which create networks of nodes (or virtual neurons), have also been recently reported [19,20] for their ability to demonstrate complex processing tasks (e.g. prediction and classification) with optical signals.

In the development of future PNNs, the weighting of inputs via photonic synaptic connections will be crucial to the flow of information, with each weight controlling the strength of an input to the subsequent layer. Photonic weights therefore represent the trainability of PNNs and are a crucial step in functional operations such as multiply and accumulate (MAC), used by widely deployed convolutional neural networks, to perform image processing. Recent photonic approaches to photonic synapses have seen the use of different systesms, including PCMs [21,22] and microring resonators [23,24]. However, only very recently photonic synaptic weighting has been experimentally demonstrated with VCSELs [25], following a number of theoretical reports of VCSELs as ideal candidates for neuromorphic photonic spiking neurons and synaptic elements [26,27]. Specifically, in [25] a photonic VCSEL-based synaptic system was demonstrated permitting the fast (GHz rates) weighting and dynamical weight tuning of incoming optical spikes. This used a VCSEL biased below its lasing threshold and operating as a vertical cavity semiconductor optical amplifier (VCSOA), thanks to the intrinsic non-linear gain of such systems under optical injection [28]. This work reports experimentally on the scalability of VCSEL-based photonic synapses in basic network configurations (in series and in parallel) for the realization of all optical systems capable of neural network processing operations with fast (GHz rates) and low power (tens of μWs) optical spiking signals. Here, we demonstrate experimentally that using two in-series interconnected photonic VCSEL-based synapses, sequential weights can be applied to fast (150 ps long and possibly faster) spikes. Moreover, we show that using two photonic VCSEL-based synapses in a parallel architecture allows for the realization of MAC operations with fast optical spiking. In the two investigated photonic synapse architectures (in-series and in-parallel) we additionally demonstrate the capability to apply user defined, time-dependent weights to trains of optical input pulses (spikes), with fast weight tunability demonstrated here up to 500 MHz (although faster operation is expected). This is achieved through the simple mechanism of tuning the bias current applied to the off-the-shelf, telecom-compatible (1300 & 1550 nm) VCSELs used throughout this work.

2. Experimental setup

Figures 1(a)–1(b) show the experimental setups used in this work to investigate the operation of VCSEL-based synaptic systems in series (Fig. 1(a)) and in parallel architectures (Fig. 1(b)). In our approach, the VCSELs were biased below their lasing threshold current (I_{th}) and operated as vertical cavity semiconductor optical amplifiers (VCSOAs). Firstly, to create the in series VCSOA synaptic system (Fig. 1(a)), a 1300 nm tuneable laser (TL) was used to inject light into two commercially-sourced (Raycan) 1300 nm VCSOAs. The TL signal was passed through an optical isolator (ISO), a variable optical attenuator (VOA), and a polarization controller before being introduced into a Mach-Zehnder modulator (MZM). A pulse generator (PG) was used, along with the MZM, to modulate the TL's injection to produce 200 ps pulses at a 15 MHz repetition rate. The optical signal was then polarization matched to the VCSEL's parallel resonant mode, using a polarization controller (PC), and divided into two paths using a 50/50 splitter. The first branch was directed to a power meter (PM) for input power monitoring, and the second one was connected to a commercially-sourced (RayCan) 1286 nm VCSEL (VCSOA-1, I_{th} = 0.79 mA at 293 K), biased below threshold (<95% I_{th}), for optical injection via an optical circulator (CIRC).

Optical Materials EXPRESS

The output of the first VCSOA was collected by the CIRC and propagated into a second VCSEL (VCSOA-2, I_{th} = 1.39 mA at 293 K). VCSOA-1 was polarization matched to VCSOA-2's parallel transverse mode using a PC, and the wavelength of the devices was matched by changing the temperature of VCSOA-2. The spectra of the TL, VCSOA-1 and VCSOA-2 are shown in Fig. 1(c), where both VCSOA's main resonant peak overlap and the TL peak is slightly detuned, with a set initial frequency detuning between the TL and the VCSOAs (Δf) equal to −3.6 GHz. Finally, VCSOA-2's output was measured by a photodectetor (PD) and the collected time traces were recorded by a fast 8 GHz real-time oscilloscope (SCOPE). The in series VCSOA-based photonic synapses were operated with both static and dynamic weights. Static weighting was achieved by configuring the bias current of the VCSOAs to achieve a specific weighting of the injected optical pulses. Dynamic (time-varying) weighting was achieved using a 2-channel arbitrary waveform generator (AWG) to controllably modulate the bias currents of both VCSOAs via integrated 500 MHz-frequency bias tees. The experimental setup depicted in Fig. 1(b) shows in turn the setup used to investigate in parallel VCSOA synaptic systems for weight and sum (multiply and accumulate, MAC) operations on incoming fast optical pulses (or spikes). Two tuneable laser (TL) sources at two distinct wavelengths (1286 nm and 1549 nm) were intensity modulated with fast 200 ps-long pulses from a 15 MHz pulse generator. The 1286 nm branch injected pulses into VCSOA-1 (I_{th} = 0.79 mA at 293 K) and the 1549 nm branch injected pulses into VCSOA-2 (I_{th} = 1.86 mA at 293 K). The incoming optical pulses at each wavelength were

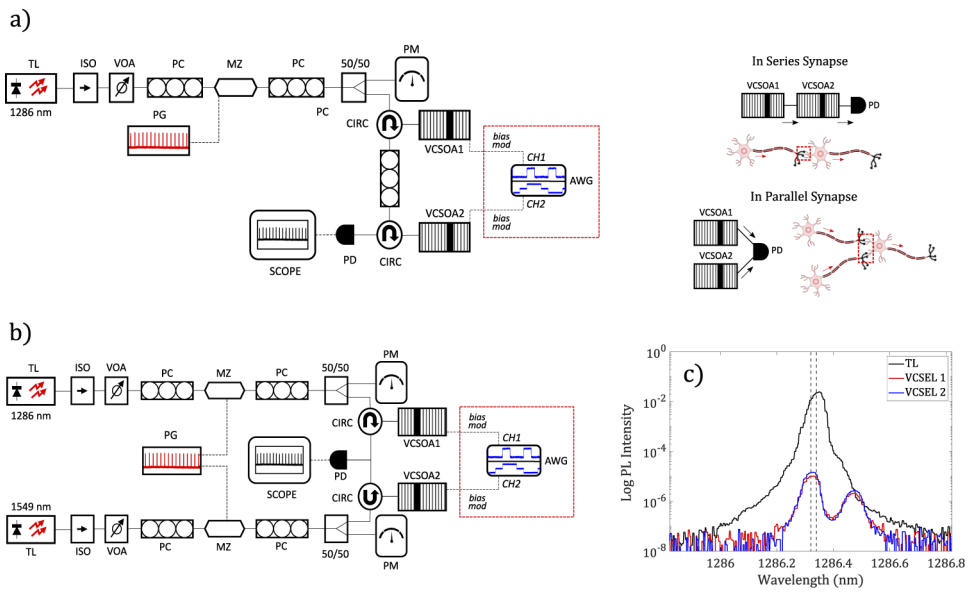

Fig. 1. Schematic description of the experimental setups used for the a) in series and b) in parallel VCSOA-based synaptic systems, consisting of: a tunable laser (TL), optical isolator (ISO), variable optical attenuator (VOA), polarization controller (PC), Mach-Zehnder modulator (MZM), pulse generator (PG), two-channel arbitrary waveform generator (AWG), power meter (PM), 50/50 splitter, optical circulator (CIRC), photodetector (PD) and oscilloscope (SCOPE). During dynamic weighting, AWG channel one (CH1) modulated VCSOA-1 bias current and channel 2 (CH2) modulated VCSOA-2 bias current. c) Measured optical spectra of the TL's injection (black) and the free-running VCSEL-1 (blue) & VCSEL-2 (red) used in a). The VCSELs are polarization matched and the TL's peak is detuned by −3.6 GHz. VCSEL diagrams demonstrate the 1-to-1 (in series) and 2-to-1 (in parallel) photonic synaptic systems that emulate neuronal synapse.

Optical Materials EXPRESS

weighted according to the operation point of the VCSOAs and then combined in a fast 9 GHz amplified photodetector before analysis. For the in parallel architecture, the weighting of the pulses could again be static (a single constant weight) or dynamic (varying in time). The latter was achieved using the components in the red highlighted box (Fig. 1(b)), where custom AWG signals were used to modulate the bias currents of the two parallel VCSOAs. Input pulses were therefore multiplied by a configurable weight before all parallel branches were added (irrespective of their wavelength) in the photodetector.

3. Results and discussion

3.1. In series VCSOA synapse for weight and amplitude control

Figure 2(a) shows the characterization results for VCSOA-1 and VCSOA-2 connected in series. First, VCSOA-1 was biased at 1.31 mA (~95% I_{th}) while a constant subthreshold current of 0.64 to 0.74 mA was varied across VCSOA-2. The top plot of Fig. 2(a) (red) shows the incoming TL input signal, consisting of 150 ps-long pulses at a 0.5 GHz repetition rate. The resultant time series, recorded at the output of VCSOA-2, are plotted in black for the constant bias current values of 0.65 and 0.74 mA respectively. These show that fast (150 ps-long) input pulses can be weighted and propagated in a feed-forward architecture from one VCSOA to another. The average measured pulse peak power at the output of VCSOA-2 (for the full current range applied to VCSOA-2) is plotted in Fig. 2(b). The latter shows that the weight of the optical pulses can be tuned with a 8.2-bit accuracy (range divided by maximum error, [25,29]), corresponding to a dynamic range of 18.3 dB, simply by acting on the bias current applied to VCSOA-2. Fig. 2(a) also plots (in grey) similar results for the case of constant current across VCSOA-2 and a varying current across VCSOA-1. In this experiment VCSOA-2 was operated at 0.73$\dot{m}$A (~95% I_{th}) and VCSOA-1 was swept from 1.21 to 1.31 mA. The time series measured at the output of VCSOA-2 show the output pulses associated with a VCSOA-1 bias of 1.21, and 1.31 mA. In this case, VCSOA-1 performed the weighting of pulses (controlled by the applied bias current) before propagating output pulses into VCSOA-2 (which applied a constant weight). It was found that the output pulses can be tuned with a 7-bit accuracy (16.9 dB) by acting on the bias current of VCSOA-1. These first results show the ability of in series synapses to propagate short optical pulses (or spikes) from one synapse to another and to successfully apply controlled cascaded weights to incoming pulsating (spiking) signals. The bit accuracy achieved with these devices allows us to produce multiple distinguishable weights, matching the performance of similar photonic weighting systems based on PCMs [30] and microring weight banks [29].

We also show that the in series VCSOA synaptic system can perform the dynamic weight control of fast optical pulses (spikes) at high speed. For this experiment, we modulated the current of VCSOA-1 with a 3 level signal (using the AWG), creating a time-dependent weighting pattern with multiple discrete levels $W_1 \rightarrow W_3$ (see Fig. 2(c)). We again used the AWG to modulate the TL with 150 ps pulses at repetition rate of 0.5 GHz. The current of VCSOA-2 was configured with different constant values ranging from 0.68 to 0.73 mA. Fig. 2(c) includes the output traces associated with VCSOA-2's selected applied current, showing that the propagated pulses followed the weights assigned by VCSOA-1. Additionally, the collective output intensity of the pulses can be tuned by simply varying VCSOA-2's driving current. This functionality realizes the ability to dynamically apply a diverse set of weights to individual pulses, before controlling the final output amplitude with the second VCSOA. Such a two-stage weight-and-control operation would allow for the attenuation of strong node outputs in spiking neural network (SNN) layers as well as permit compensation of losses given its ability to further amplify signals.

Next, we dynamically modulated the current applied to the two VCSOAs within the in series synaptic system simultaneously. To do so, we used signals generated by the two channels of the AWG. The TL injection was in turn modulated with a PG, generating 200 ps optical pulses (see Fig. 2(d)) at 15 MHz (limited by the PG's maximum repetition rate). Here, VCSOA-1's

Optical Materials EXPRESS

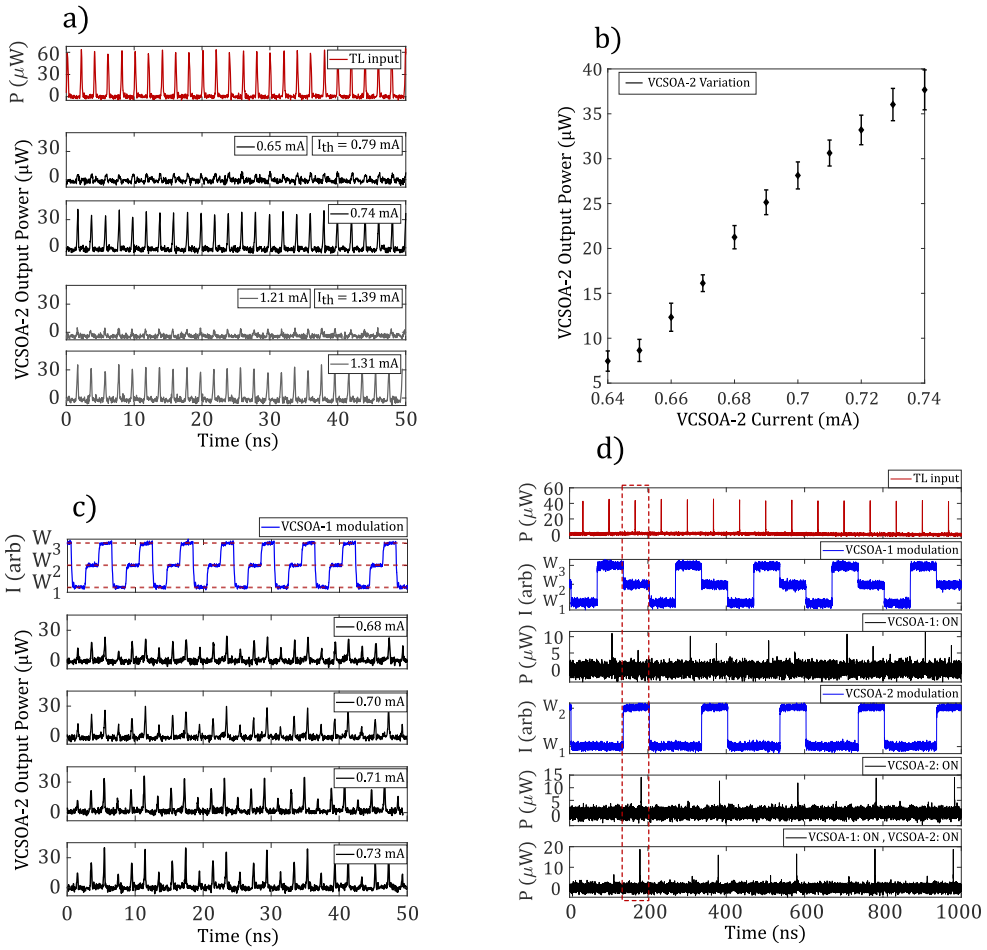

Fig. 2. a) Time series of the TL input signal (red), consisting of 150 ps pulses at 0.5 GHz, and the measured optical output at VCSOA-2, for various constant bias currents, VCSOA-2 (black, $I = 0.65 \rightarrow 0.74\,mA$) and VCSOA-1 (grey, $I = 1.21 \rightarrow 1.31\,mA$). The threshold current of each VCSEL (I_{th}) is highlighted. b) The corresponding average pulse peak power as a function of applied bias current for VCSOA-2 ($I = 0.64 \rightarrow 74\,mA$), showing a 8.2 bit-accuracy and 18.3 dB dynamic range. c) Dynamic 3 level modulation of VCSOA-1's bias current with distinct weights $W_1 \rightarrow W_3$ and the resultant output for multiple configured VCSOA-2 bias currents. d) Simultaneous dynamic modulation of VCSOA-1 and VCSOA-2. The TL input (red), the modulation signals (blue) and the corresponding measured outputs (black) are shown, revealing the ability to apply accumulative weights and temporally filter input pulses.

current was modulated using another 3 level signal, where each level was assigned a distinct weight $W_1 \rightarrow W_3$, alternating every 66 ns. VCSOA-2 was modulated with a single 66 ns square perturbation, introduced every 200 ns (approx. 3 x 66 ns). Fig. 2(d) includes the system's output when VCSOA-2's modulation was switched off (i.e. driven at a constant current just below 95% I_{th}). The output trace shows the input pulses weighted by VCSOA-1 are propagated to VCSOA-2, yielding output pulses with three distinct (weighted) amplitudes. Inversely, when VCSOA-1's (VCSOA-2) modulation was switched off (on), the input signal was propagated through VCSOA-1 before adhering to the weights applied by VCSOA-2. Finally, Fig. 2(d) shows

Optical Materials EXPRESS

the measured output when both VCSOA modulations were switched on simultaneously. The resulting system output shows a combination of the weights set in VCSOA-1 and VCSOA-2, with the amplitude of the selected pulses (dashed-red highlight) seeing an average amplification enhancement of ~2.6 when weight W_2 was applied by VCSOA-2. Additionally, non-target optical pulses were effectively inhibited by the application of the lower VCSOA-2 weight W_1. Thus, this result shows that the in series VCSOA synaptic system can sequentially apply dynamic weights to fast incoming optical pulses and successfully apply accumulative weights to signals between the two VCSOAs. For example, this permits the dynamical encoding of information onto individual pulses within a pulse train, as well as the application of individual dynamical weights to each pulse. Additionally, different weight combinations can allow for the temporal filtering of input signals.

3.2. Parallel VCSOA synapse for MAC operations

To investigate the in parallel VCSOA synapse system and its potential to perform MAC operations, we used the experimental setup included in Fig. 1(b). In our first demonstration, the two parallel VCSOAs (operating and 1300 nm and 1550 nm) were used to statically weight the 150 ps-long pulses injected into each device at their respective wavelengths. VCSOA-1 and VCSOA-2 were biased with constant currents configured to give distinct weight values $W_{v1}3$ & $W_{v2}3$. These weight values provided the maximum amplification of the 21 μW (1286 nm) and 25 μW (1550 nm) optical pulses (spikes) injected into each device. The in parallel operation was therefore demonstrated with smaller input pulses than those used in the previous in series demonstration. $W_{v1}3$ was set by selecting a bias current of 0.767 mA in VCSOA-1 and $W_{v2}3$ was set by selecting a bias current of 1.791 mA in VCSOA-2. As shown in Fig. 3(a), $W_{v1}3$ successfully produced 31 μW (~1.5 amplification factor) output pulses at VCSOA-1 (red) and $W_{v2}3$ produced 29 μW (~1.2 amplification factor) output pulses at VCSOA-2 (blue). The signal collected by the photodetector at the system's output, plotted in Fig. 3(a) (black), revealed that an output pulse of 62 μW was obtained after the combination of both VCSOA synapses. This value correlates to the summation of the two weighted pulses, $W_{v1}3$ & $W_{v2}3$, therefore realizing the MAC operation ($W_{v1}3$ x *Input*) + ($W_{v2}3$ x *Input*). Testing the system further, the weight applied by VCSOA-1 was then slowly decreased, with that applied to VCSOA-2 remaining unchanged. The results in Fig. 3(b)–3(c) show that the amplitude of the 1286 nm weighted pulse decreased to 23 μW at $W_{v1}2$ (I = 0.707 mA) and 5 μW at $W_{v1}1$ (I = 0.606 mA). The subsequent MAC output, captured by the photodetector, again correctly produced the summed output, revealing pulses with amplitudes of 52 μW and 34 μW.

Following the demonstration of the MAC operation with the in parallel VCSEL photonic synapse, the experiment was repeated for variations of VCSOA-2's weight (see Fig. 3(d)–3(f)). Here, VCSOA-1 was configured with a constant bias current (I = 0.767 mA) while the weight applied by VCSOA-2 was decreased from $W_{v2}3$ (I = 1.791 mA) to $W_{v2}1$ (I = 1.673 mA). The results of the MAC operation, measured at the photodetector, successfully showed the summation of the weighted pulses according to (W_{v1} x *Input*) + (W_{v2} x *Input*). The results in Fig. 3 demonstrate that static weights, applied to parallel VCSOA synapses, can be used to perform MAC operations with low input powers (pulse peak powers of only a few tens of μW) and very small changes in applied bias current (tens of μA). Furthermore, the system can perform MAC operations at high speed rates with only an upper limit on the frequency of input data. This limitation on input speed is set by the recovery time of the VCSOAs and is determined by the carrier lifetime, which for the case of the commercially sourced VCSELs used in this work is typically ~1 ns. Therefore, the proposed VCSOA synapse, using off the shelf devices without any additional device optimization stages, easily enables up to GHz operation. Furthermore, the wavelength-independent photodetector response (over the used range of wavelengths) allows for combination of signals across a diverse range of wavelengths, thus enabling wavelength agnostic

Optical Materials EXPRESS

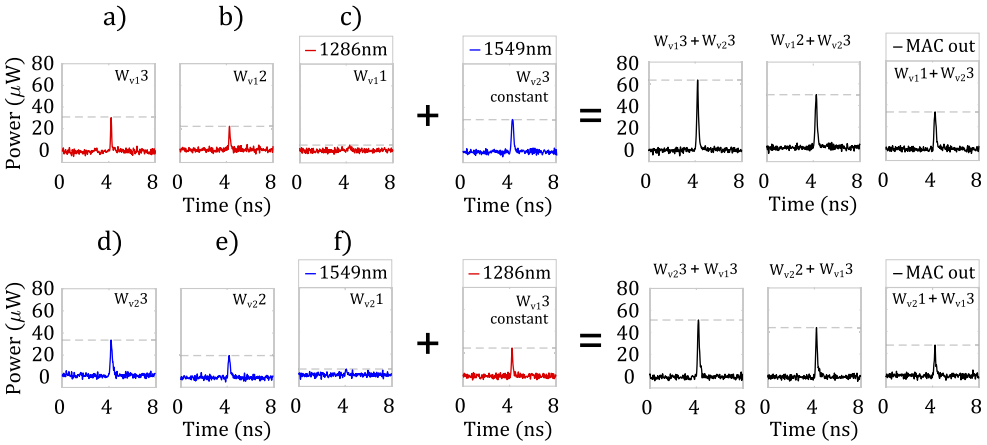

Fig. 3. Multiply and accumulate (MAC) operation with the static weighting of 1286 nm (red) and 1549 nm (blue) input pulses. The resultant MAC output (black) is collected directly by a photodetector. a) & d) Max pulse weights were configured using bias current of 0.767 mA and 1.791 mA for VCSOA-1 and VCSOA-2 respectively. The weight of VCSOA-1 was reduced incrementally to b) 0.707 mA & c) 0.606 mA, with the weight of VCSOA-2 constant. We refer to the weights of VCSOA-1 as $W_{v1}3 \rightarrow W_{v1}1$ and the weight of VCSOA-2 as $W_{v2}3$. The weight of VCSOA-1 was kept constant ($W_{v1}3$) and the weight of VCSOA-2 was reduced incrementally from maximum to e) 1.753 mA & f) 1.673 mA. We refer to the weights of VCSOA-2 as $W_{v2}3 \rightarrow W_{v2}1$.

operation and the use of non-identical VCSEL devices. This makes for a highly hardware friendly, low power and high-speed system where parallel photonic synapses can be scaled up to larger platforms, using for example integrated VCSEL-arrays, for a high number of devices on a single chip. The potential application of diffractive optical elements [31] or microlens arrays [32] in combination with VCSEL arrays, could allow us to route signals to individual devices and achieve parallel processing or even dot-product operations, like those key to implementing future processing systems based upon spiking PNNs.

Dynamic weighting can also replace static weighting in the in parallel VCSOA synapse for high speed on-the-fly adjustments. This remote control of synaptic weights would allow for future systems based upon the in parallel VCSEL synapses, to quickly adapt to a new task or training set without the need for manual parameter setting. Therefore, in Fig. 4 we used two parallel VCSOAs with dynamic (time-varying) weights. Using the AWG we generated two distinct signals to modulate the bias of each VCSOA, a 2 level signal (VCSOA-1) and a 3 level signal (VCSOA-2), respectively (Figs. 4(a)–4(b) (blue)). Again, an optical signal encoded with 200 ps input pulses at a repetition rate of 15 MHz (produced using a PG) was injected into the two parallel VCSOAs, as shown in Figs 4(a)–4(b) (red). The pulses generated at the output of VCSOA-1 (Fig. 4(a), black) had two amplitude levels corresponding to the weights, $W_{v1}2$ and $W_{v1}1$. The alternating weights produced attenuated and amplified pulses according to the modulation signal. The results of VCSOA-2, shown in Fig. 4(b), produced a similar effect with three output pulse weights, $W_{v2}3$, $W_{v2}2$ and $W_{v2}1$. The combined weighted pulse trains in Fig. 4(c) show the output of the MAC operation. We note that here the two output signals were combined offline during post processing. In Fig. 4(c), we see that six levels of output pulse amplitude are produced. This is the expected result as each output level corresponds to one of the possible weight combinations ($W_{v1}1 + W_{v2}3$, $W_{v1}1 + W_{v2}2$, $W_{v1}1 + W_{v2}1 \ldots$). Due to the similarities in VCSOA amplification and injected input pulses, we found that weight combinations of $W_{v1}1 + W_{v2}3$ and $W_{v1}2 + W_{v2}2$ produce similar MAC output pulses. This is expected as many weight combinations can produce similar

Optical Materials EXPRESS

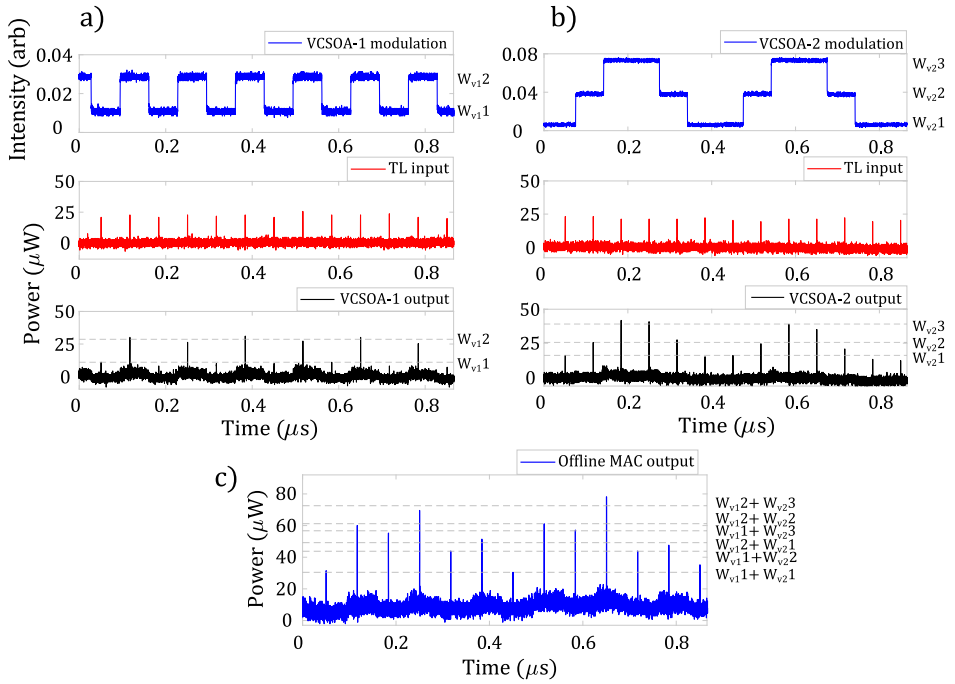

Fig. 4. Parallel dynamic weighting and MAC output. AWG signal (blue) is used to dynamically weight the VCSOA output. Input pulses (red) were injected at a rate of 15 MHz into both parallel VCSOAs. The output of each VCSOA is plotted in black. The results for a) 1286 nm and b) 1549 nm VCSOAs are then combined to provide a c) MAC output. The MAC output is calculated offline.

results. Overall, weight and sum operations with fast optical pulses can be performed by parallel VCSOA synapses with high speed and user defined weight control. By combining in series and in parallel VCSOA synapse configurations, the functionality of both demonstrations could be brought together, creating a system with access to parallel input encoding, input weighting, and wavelength-independent summation. This VCSOA-based approach is therefore well suited for adjustable weight control in future photonic neuronal networks, including light-enabled Spiking Neural Networks (SNNs).

4. Conclusion

We demonstrate experimentally that VCSEL-based artificial synapses, built in serial and parallel configurations, successfully yield ultrafast spike processing systems (spike amplification/suppression, weighting or MAC operations) for use in future photonic-enabled neural networks including SNNs. We show that an in series dual VCSOA photonic architecture can first apply configurable weights to individual fast (200 ps) optical pulses (spikes), before providing further attenuation/amplification and yielding a temporally-resolved, weighted (and filtered) optical spiking signal at its output. Moreover, thanks to the weighting values achieved of up to 1.5 (thus providing amplification), network-incorporated VCSOA synapses would allow for the adjustment of signal levels and the beneficial compensation of signal loss in subsequent network layers in photonic SNNs. Furthermore, this work also demonstrates that in-parallel VCSOA-based synaptic systems can perform weight and sum (multiply and accumulate, MAC) operations. This has great implications for the future realization of VCSEL-based neuromorphic

Optical Materials EXPRESS

processing systems able to perform parallel processing tasks like convolution, as well as the completion of mathematical functions like dot products. In both the in series and in parallel VCSEL-based photonic synaptic configurations, we demonstrated operation with high speed (down to 150 ps long, and possibly lower), low power (a few tens of μWs) optical pulses (spikes). Additionally in each investigated configuration, we demonstrated high speed dynamic weighting capability through the modulation of applied bias current; hence permitting the fast and remote tuning of synaptic weights. This enables our proposed photonic synaptic hardware to be easily readjusted for different network tasks or training cycles. Additionally, all our experiments are achieved with commercially-sourced VCSELs and fibre-optic components at key telecommunication wavelengths (1300 and 1550 nm); thus making our approach fully compatible with optical communication networks and data centre technologies. This work therefore highlights the potentials of VCSEL-based photonic synapses for the implementation of hardware friendly, low-power, high-speed and fast-tuning weight control platforms for use in future neuromorphic photonic spike processing platforms.

Funding. European Commission (828841-ChipAI-H2020-FETOPEN-2018-2020); Engineering and Physical Sciences Research Council (EP/N509760/1, EP/P006973/1); Office of Naval Research Global (ONRG-NICOP-N62909-18-1-2027); UK Research and Innovation (EP/V025198/1).

Disclosures. The authors declare no conflicts of interest.

Data availability. All data underpinning this publication are openly available from the University of Strathclyde KnowledgeBase [33].

References

1. E. Callaway, "It will change everything': DeepMind's AI makes gigantic leap in solving protein structures," Nature **588**(7837), 203–204 (2020).
2. M. Davies, N. Srinivasa, T.-H. Lin, G. Chinya, Y. Cao, S. H. Choday, G. Dimou, P. Joshi, N. Imam, S. Jain, Y. Liao, C.-K. Lin, A. Lines, R. Liu, D. Mathaikutty, S. McCoy, A. Paul, J. Tse, G. Venkataramanan, Y.-H. Weng, A. Wild, Y. Yang, and H. Wang, "Loihi: a neuromorphic manycore processor with on-chip learning," IEEE Micro **38**(1), 82–99 (2018).
3. M. V. DeBole, R. Appuswamy, P. J. Carlson, A. S. Cassidy, P. Datta, S. K. Esser, G. J. Garreau, K. L. Holland, S. Lekuch, M. Mastro, J. McKinstry, B. Taba, C. di Nolfo, B. Paulovicks, J. Sawada, K. Schleupen, B. G. Shaw, J. L. Klamo, M. D. Flickner, J. V. Arthur, D. S. Modha, A. Amir, F. Akopyan, A. Andreopoulos, W. P. Risk, J. Kusnitz, C. Ortega Otero, and T. K. Nayak, "TrueNorth: accelerating from zero to 64 million neurons in 10 years," Computer **52**(5), 20–29 (2019).
4. S. Friedmann, J. Schemmel, A. Grübl, A. Hartel, M. Hock, and K. Meier, "Demonstrating hybrid learning in a flexible neuromorphic hardware system," IEEE Trans. Biomed. Circuits Syst. **11**(1), 128–142 (2017).
5. J. Shalf, "The future of computing beyond Moore's Law," Philos. Trans. R. Soc., A **378**(2166), 20190061 (2020).
6. D. A. B. Miller, "Attojoule optoelectronics for low-energy information processing and communications," J. Lightwave Technol. **35**(3), 346–396 (2017).
7. J. Feldmann, N. Youngblood, C. D. Wright, H. Bhaskaran, and W. H. Pernice, "All-optical spiking neurosynaptic networks with self-learning capabilities," Nature **569**(7755), 208–214 (2019).
8. A. Mehrabian, Y. Al-Kabani, V. J. Sorger, and T. El-Ghazawi, "Pcnna: A photonic convolutional neural network accelerator," in *2018 31st IEEE International System-on-Chip Conference (SOCC)*, (2018), pp. 169–173.
9. X. Xu, M. Tan, B. Corcoran, J. Wu, A. Boes, T. G. Nguyen, S. T. Chu, B. E. Little, D. G. Hicks, R. Morandotti, A. Mitchell, and D. J. Moss, "11 TOPS photonic convolutional accelerator for optical neural networks," Nature **589**(7840), 44–51 (2021).
10. V. A. Pammi, K. Alfaro-Bittner, M. G. Clerc, and S. Barbay, "Photonic computing with single and coupled spiking micropillar lasers," IEEE J. Sel. Top. Quantum Electron. **26**(1), 1–7 (2020).
11. G. Sarantoglou, M. Skontranis, and C. Mesaritakis, "All optical integrate and fire neuromorphic node based on single section quantum dot laser," IEEE J. Sel. Top. Quantum Electron. **26**(5), 1–10 (2020).
12. P. R. Prucnal, B. J. Shastri, T. F. de Lima, M. A. Nahmias, and A. N. Tait, "Recent progress in semiconductor excitable lasers for photonic spike processing," Adv. Opt. Photonics **8**(2), 228–299 (2016).
13. J. Robertson, M. Hejda, J. Bueno, and A. Hurtado, "Ultrafast optical integration and pattern classification for neuromorphic photonics based on spiking VCSEL neurons," Sci. Rep. **10**(1), 6098 (2020).
14. J. Robertson, P. Kirkland, J. A. Alanis, M. Hejda, J. Bueno, G. Di Caterina, and A. Hurtado, "Ultrafast neuromorphic photonic image processing with a VCSEL Neuron," arXiv (2021).
15. T. Deng, J. Robertson, and A. Hurtado, "Controlled propagation of spiking dynamics in vertical-cavity surface-emitting lasers: towards neuromorphic photonic networks," IEEE J. Sel. Top. Quantum Electron. **23**(6), 1–8 (2017).

Optical Materials EXPRESS

16. T. Deng, J. Robertson, Z.-M. Wu, G.-Q. Xia, X.-D. Lin, X. Tang, Z.-J. Wang, and A. Hurtado, "Stable propagation of inhibited spiking dynamics in vertical-cavity surface-emitting lasers for neuromorphic photonic networks," IEEE Access **6**, 67951–67958 (2018).
17. M. Hejda, J. Robertson, J. Bueno, J. A. Alanis, and A. Hurtado, "Neuromorphic encoding of image pixel data into rate-coded optical spike trains with a photonic VCSEL-neuron," APL Photonics **6**(6), 060802 (2021).
18. Y. Zhang, J. Robertson, S. Xiang, M. Hejda, J. Bueno, and A. Hurtado, "All-optical neuromorphic binary convolution with a spiking VCSEL neuron for image gradient magnitudes," Photonics Res. **9**(5), B201 (2021).
19. J. Vatin, D. Rontani, and M. Sciamanna, "Experimental reservoir computing using VCSEL polarization dynamics," Opt. Express **27**(13), 18579 (2019).
20. J. Bueno, J. Robertson, M. Hejda, and A. Hurtado, "Comprehensive performance analysis of a VCSEL-based photonic reservoir computer," IEEE Photonics Technol. Lett. **33**(16), 920–923 (2021).
21. J. Feldmann, N. Youngblood, M. Karpov, H. Gehring, X. Li, M. L. Gallo, X. Fu, A. Lukashchuk, A. S. Raja, J. Liu, C. D. Wright, A. Sebastian, T. J. Kippenberg, W. H. Pernice, and H. Bhaskaran, "Parallel convolution processing using an integrated photonic tensor coer," Nature **589**(7840), 52–58 (2021).
22. J. Wang, L. Wang, and J. Liu, "Overview of phase-change materials based photonic devices," IEEE Access **8**, 121211–121245 (2020).
23. A. N. Tait, T. Ferreira de Lima, M. A. Nahmias, B. J. Shastri, and P. R. Prucnal, "Continuous calibration of microring weights for analog optical networks," IEEE Photonics Technol. Lett. **28**(8), 887–890 (2016).
24. A. N. Tait, T. Ferreira de Lima, M. A. Nahmias, H. B. Miller, H.-T. Peng, B. J. Shastri, and P. R. Prucnal, "Silicon photonic modulator neuron," Phys. Rev. Appl. **11**(6), 064043 (2019).
25. J. A. Alanis, J. Robertson, M. Hejda, and A. Hurtado, "Weight adjustable photonic synapse by nonlinear gain in a vertical cavity semiconductor optical amplifier," Appl. Phys. Lett. **119**(20), 201104 (2021).
26. S. Xiang, Y. Zhang, J. Gong, X. Guo, L. Lin, and Y. Hao, "STDP-based unsupervised spike pattern learning in a photonic spiking neural network with VCSELs and VCSOAs," IEEE J. Sel. Top. Quantum Electron. **25**(6), 1–9 (2019).
27. T. Tian, M. Ni, Zhengmao, W. Guangqiong, X. Xiaodong, and L. Tao Deng, "Theoretical investigation of weight-dependent optical spike timing dependent plasticity based on VCSOA," J. Phys.: Conf. Ser. **1792**(1), 012037 (2021).
28. A. Hurtado, I. D. Henning, and M. J. Adams, "Bistability and nonlinear gain in 1.55μm vertical cavity semiconductor optical amplifiers: theory and experiments," Appl. Phys. Lett. **91**(15), 151106 (2007).
29. A. N. Tait, T. F. de Lima, M. A. Nahmias, B. J. Shastri, and P. R. Prucnal, "Multi-channel control for microring weight banks," Opt. Express **24**(8), 8895 (2016).
30. Z. Cheng, C. Ríos, W. H. P. Pernice, C. D. Wright, and H. Bhaskaran, "On-chip photonic synapse," Sci. Adv. **3**(9), 1 (2017).
31. T. Heuser, M. Pflüger, I. Fischer, J. A. Lott, D. Brunner, and S. Reitzenstein, "Developing a photonic hardware platform for brain-inspired computing based on 5 × 5 VCSEL arrays," JPhys Photonics **2**(4), 044002 (2020).
32. J. Lim, S.-m. Kim, S. Kang, J. Han, and H. Kim, "Design and fabrication of microlens array for VCSEL to fiber coupling," in *Optifab 2005: Technical Digest*, (SPIE, 2005), p. 30.
33. J. Robertson and J. A. Alanis, "Photonic synaptic system for MAC operations by interconnected vertical cavity surface emitting lasers: data," University of Strathclyde KnowledgeBase, 2022, https://doi.org/10.15129/b4f4d8ce-4282-49e5-8978-82b92c52aa0d.